ELSEVIER

Biochimica et Biophysica Acta 1515 (2001) 101–109

BIOCHIMICA ET BIOPHYSICA ACTA
BBA

www.bba-direct.com

Cargo delivery kinetics of cell-penetrating peptides

Mattias Hällbrink [a,c], Anders Florén [a,c], Anna Elmquist [a,c], Margus Pooga [b], Tamas Bartfai [c], Ülo Langel [a,c,*]

[a] *Department of Neurochemistry and Neurotoxicology, Arrhenius Laboratories, Stockholm University, S-10691 Stockholm, Sweden*
[b] *Estonian Biocentre, 23 Riia Street, EE-51010 Tartu, Estonia*
[c] *The Harold L. Dorris Neurological Research Center, Department of Neuropharmacology, The Scripps Research Institute, 10550 North Torrey Pines Road, La Jolla, CA 92037, USA*

Received 17 November 2000; received in revised form 24 July 2001; accepted 24 July 2001

Abstract

A diversity of cell-penetrating peptides (CPPs), is known, but so far the only common denominator for these peptides is the ability to gain cell entry in an energy-independent manner. The mechanism used by CPPs for cell entry is largely unknown, and data comparing the different peptides are lacking. In order to gain more information about the cell-penetrating process, as well as to quantitatively compare the uptake efficiency of different CPPs, we have studied the cellular uptake and cargo delivery kinetics of penetratin, transportan, Tat (48–60) and MAP (KLAL). The respective CPPs (labelled with the fluorescence quencher, 3-nitrotyrosine) are coupled to small a pentapeptide cargo (labelled with the 2-amino benzoic acid fluorophore) via a disulfide bond. The cellular uptake of the cargo is registered as an increase in fluorescence intensity when the disulfide bond of the CPP–S–S–cargo construct is reduced in the intracellular milieu. Our data show that MAP has the fastest uptake, followed by transportan, Tat(48–60) and, last, penetratin. Similarly, MAP has the highest cargo delivery efficiency, followed by transportan, Tat (48–60) and, last, penetratin. Since some CPPs have been found to be toxic at high concentration, we characterized the influence of CPPs on cellular 2-[^{3}H]deoxyglucose-6-phosphate leakage. Measurements on this system show that the membrane-disturbing potential appears to be correlated with the hydrophobic moment of the peptides. In summary, the yield and kinetics of cellular cargo delivery for four different CPPs has been quantitatively characterized.

Keywords: Cell-penetrating peptides; Cellular uptake; Cargo delivery kinetics

1. Introduction

During the last 10 years, several peptides have been demonstrated to translocate across the plasma membrane of eukaryotic cells by a seemingly energy-independent pathway, i.e. they internalize even when cells are incubated at 4°C. These peptides have been used for transmembrane delivery of hydrophilic macromolecules. Cellular delivery using cell-penetrating peptides, CPPs, offer several advantages over con-

Abbreviations: Abz, 2-amino benzoic acid (anthranilic acid); CPP, cell-penetrating peptide; DTT, dithiothreitol; HKR, HEPES-buffered Krebs–Ringer solution; μ, hydrophobic moment; MAP, model amphipathic peptide; NLS, nuclear localization signal

* Corresponding author. Fax: +46-8-161371.
E-mail address: ulo@neurochem.su.se (U. Langel).

0005-2736/01/$ – see front matter
PII: S0005-2736(01)00398-4

ventional techniques, as it is efficient for a range of cell types and can be applied to cells en masse. Thus, CPPs can be used as delivery vectors for pharmacologically interesting substances, such as antisense oligonucleotides, proteins and peptides. For review see Lindgren et al., [1].

CPPs have been found to have toxic effects at higher concentrations, probably due to lytic properties [2]. Hence, it is of importance to investigate the influence of these peptides on membrane integrity. In addition, indication of the type of CPP that should be used for a particular application would be facilitated if their cargo delivery kinetics and efficacy were known.

Here we compare the uptake and cargo delivery efficiency as well as the membrane-disturbing properties of four different CPPs: penetratin [3], Tat (48–60) [4], transportan [5], and model amphipathic peptide (MAP) [6] (table 1). Penetratin, or antennapedia (43–58), is a 16-amino acid long peptide corresponding to the third helix of the *Antennapedia* homeodomain deprived of its N-terminal glutamate (table 1). The peptide and analogues have been used for transmembrane delivery of a diversity of hydrophilic macromolecules, for review of penetratins see Derossi et al. [7].

Tat (48–60) (table 1), encompasses the whole basic region and nuclear localization signal (NLS) of the HIV trans activating factor protein Tat. The NLS is not sufficient for translocation in itself since Tat (37–53) is not taken up at all [4]. To date, more than 10 Tat-derived short peptides have been shown to translocate into the interior of different cell types. Recent reports demonstrate the use of Tat (48–60) for transmembrane transport of proteins. For review see Schwarze et al. [8].

Transportan [5], a 27-amino acid long chimeric peptide (table 1), introduced by our group, is a combination of the N-terminal fragment of the neuropeptide galanin and the membrane-interacting wasp venom peptide, mastoparan. A Lys residue connects these two bioactive peptides. Transportan has been used for intracellular delivery of peptide nucleic acids [9]. Several active and inactive analogues have been synthesized [10,11] among them the inactive [Pro^{19}]transportan which is used as a negative control in this study.

Oehlke et al. introduced an 18-mer MAP [6] (table 1) that has been used for transmembrane transport of peptides. An extensive structure–activity relationship study has been carried out [2] showing that helical amphipathicity is the most important factor for the uptake of this type of peptide.

In the present study, a short fluorophore labelled peptide, with the sequence: 2-amino benzoic acid (Abz)–Cys–LKANL, was used as cargo in the delivery measurements. The sequence was chosen at random, with the only requirement that it would be unable to translocate through the plasma membrane by itself. All four CPPs contain a Cys-residue used for covalent attachment of the cargo peptide via a disulfide bond, and a 3-nitro-tyrosine extension acting as a quencher to the Abz group, resulting in reduction sensitive constructs (Fig. 1). The disulfide bond is quickly reduced in the intracellular milieu, resulting in increased fluorescence intensity upon CPP–S–S–cargo construct internalization. Biotinylated CPPs were used for the [^{3}H]deoxyglucose-6-phosphate leakage experiments.

Based on these measurements, we propose a kinetic model for the penetration process and suggest that future designs of CPPs should aim to minimize the hydrophobic moment (μ) and thereby decrease the membrane-disturbing properties of these peptides.

2. Materials and methods

2.1. Materials

$MgCl_2$, NaCl, H_3PO_4, and EDTA were purchased from Merck, Germany, *tert*-butyloxycarbonyl (*t*-Boc)- and Fmoc-protected amino acids were from Bachem, Switzerland and Chemimpex, USA. [^{3}H]2-Deoxyglucose was purchased from NEN, USA. Cell culture media and reagents were from Gibco, USA. All other chemicals were from Sigma, St. Louis, MO, USA. Data evaluation was performed using the software Dynafit from Biokin, USA and figures were produced with GraphPad Prism 2.0 from GraphPad soft, USA.

2.2. Peptide synthesis

Peptides (cf. table 1) were synthesized in a stepwise

manner in a 0.1-mmol scale on an Applied Biosystem Model 431A peptide synthesizer on solid support using dicyclohexyl-carbodiimide/hydroxybenzotriazole activation strategy. *t*-Boc amino acids were coupled as hydroxybenzotriazole esters to a *p*-methylbenzylhydrylamine (MBHA) resin (1.1 mmol of amino groups g^{-1}, Bachem, Switzerland) to obtain C-terminally amidated peptides. Fmoc-nitro-Tyr and *t*-Boc–Cys–(NPys) or biotin were coupled manually after completion of the automatic synthesis. Deprotection of the side-chains, cleavage of the peptides and purification on HPLC were carried out as described in detail earlier [12]. The purity of the peptides was $>99\%$ as checked by HPLC analysis on Nucleosil 120–3 C_{18} column (0.4 cm$\times$10 cm). Molecular mass of each synthetic peptide was determined on a plasma desorption mass spectrometer (Bioion 20, Applied Biosystems), and the calculated values were obtained in each case.

2.3. Synthesis of disulfide fluorophore–quencher constructs

1 eq. of CPP–(nitro-Tyr)–Cys(NPys) and 1.2 eq. of free thiol containing Abz–Cys–cargo peptide was dissolved in a deoxygenated mixture of 3:2:1 DMSO/NMP/0.1 M sodium acetate, pH 4.5. The mixture was stirred for 4 h under nitrogen flow, and subsequently purified on RP-HPLC. The yield of the desired heterodimers (Fig. 1) was approximately 30%.

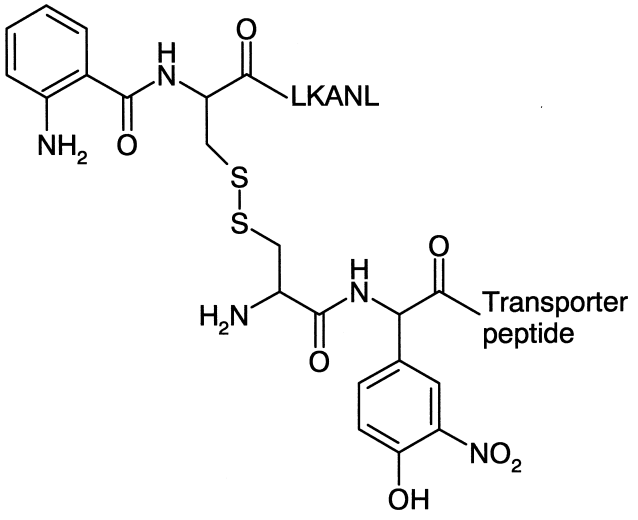

Fig. 1. The general structure of the fluoresence–quencher construct used in this study. The fluorophore-labelled cargo peptide, Abz–CLNKAL, is attached via a disulfide bond to a transporter peptide containing a 3-nitro-tyrosine, acting as quencher for Abz.

2.4. Cell cultures

Bowes human melanoma cells (American Type Culture Collection CRL-9607) were cultured in Eagle's minimal essential medium with Glutamax-I (Life Technologies, Gaithersburg, MD, USA) supplemented with 10% fetal calf serum, 1% non-essential amino acids, 1% sodium pyruvate, 100 μg ml^{-1} streptomycin, 100 U ml^{-1} penicillin. Cells for deoxyglucose leakage experiment were seeded in 12-well plates (Life Technologies, Gaithersburg, MD, USA) to a density of 70 000 cells/well in 2 ml medium. The cells were used for experiments 2 days after seeding at approximately 70–90% confluence.

Cell volume was measured in a channalyser 256 culture counter (Pharmacia, Sweden) The mean volume of Bowes melanoma cells was found to be about 1.5 pl.

2.5. Determining of reduction rate constants in the presence of lipid vesicles

10 mg of phosphatidyl choline and 5 mg of phosphatidyl serine (Sigma, Sweden) were dispersed into 1 ml of HKR by vigorous vortex mixing. The mixture was sonicated with a probe tip sonicator in 25°C for 30 min. The resulting vesicles were purified by gel filtration on Sephadex G50. The vesicles were diluted to a final concentration of 2 mg ml^{-1} in HKR. Construct was added to yield a lipid to peptide ration of about 500:1 and the mixture incubated for 10 min after which glutathione (100 μM, 500 μM, 1 mM and 2 mM) was added. Fluorescence increase was measured in a Hitachi F-2000 fluorometer and data were fitted using a numerical procedure (cf. below) to:

$$[\text{Glutathione}] + [\text{Construct}] \xrightarrow{k} [\text{Free cargo}]$$

using Dynafit software [13] (Biokin, USA).

2.6. Cellular uptake of fluorophore–quencher constructs

Cells were washed and harvested by scraping into HEPES-buffered Krebs–Ringer solution (HKR) containing 0.5 g l^{-1} glucose and counted in a Neubauer

chamber. In 96-well plates, approximately 250 000 cells in 50 μl were added to wells containing 150 μl of peptide construct dissolved in HKR to reach concentrations of 0.1, 0.5, 1, 5 or 10 μM. The cells were kept suspended by shaking between readings and the temperature was held constant at 37°C throughout the experiment. After 70 min, 5 μl 100 mM dithiothreitol (DTT) was added to reduce all remaining construct. The fluorescence intensity value obtained after DTT reduction was used to define 100%. The fluorescence intensity was found to linearly depend on construct concentration. Fluorescence was measured (ex: 320 nm, em: 420 nm) in a spectra max Gemini XS (Molecular Devices, USA) 96-well fluoro-spectrometer. After the experiment the cells were harvested by centrifugation and counted again in order to ascertain that no substantial lysis of the cells had occurred. Cells for control experiments were perforated by 5 min sonication on ice under nitrogen gas.

2.7. Fitting of the uptake of CPP–cargo constructs

In the fitting of the uptake of CPP–cargo constructs by Bowes cells we considered the reduction of the constructs in the cellular interior according to:

$$[\text{Construct}_{\text{extracellular}}] \xrightarrow{k_1} [\text{Construct}_{\text{intracellular}}] \quad (1)$$

$$[\text{Construct}_{\text{intracellular}}] + [\text{Glutathione}] \xrightarrow{k_2} [\text{Free cargo}] \quad (2)$$

To calculate the first-order rate constant for the uptake (k_1) a numerical treatment of the experimental data was applied, with the previously measured values for the second order rate constant k_2 using Dynafit software [13] (Biokin, USA). The maximum free cargo concentration was set at the concentration as endpoint. The curves for all five initial concentrations ([$\text{Construct}_{\text{extracellular}}$]) of construct were fitted simultaneously to the obtained experimental points. Consequently, the obtained values for the rate constants are valid for all curves.

2.8. Determination of intracellular glutathione concentration

Intracellular glutathione concentration was determined using a glutathione assay kit (Calbiochem, San Diego, CA, USA) according to the manufacturer's instructions.

2.9. 2-[^{3}H]Deoxyglucose-6-phosphate leakage

The glucose analogue, 2-deoxyglucose, is taken up by cells via glucose carriers and then phosphorylated by hexokinase. The product, 2-deoxyglucose-6-phosphate is not able to exit the cells through the plasma membrane [14]. The efflux of radioactivity from cells preloaded with tritium-labelled 2-deoxyglucose was measured according to the method described previously [15] with some modifications. The cells were washed with 1 ml PBS, whereupon 0.5 μCi 2-[^{3}H]deoxyglucose (Amersham, UK) in 800 μl PBS was added to preload the cells for 45 min at 37°C. Then the cells were washed rapidly three times with 1-ml portions of ice-cold PBS to remove all extracellular radioactivity. Peptides in serum-free medium

Table 1
Sequences, uptake rate constants (k_1), reduction rate constant (k_2), hydrophobic moment (μ), and equilibrium constant (K_{io}) of the CPPs used in this work

Name and sequence	k_1 (s^{-1})$\times 10^{-3}$	k_2 (M^{-1} s^{-1})	μ	(K_{io})
Penetratin *X*-RQIKIWFQNRRMKWKK-amide	0.20 ± 0.06	3.00 ± 0.04	0.091	71 ± 12
Tat (48–60) *X*-GRKKRRQRRRPQ-amide	0.34 ± 0.11	12 ± 0.2	0.073	107 ± 10
Transportan ($N^{\varepsilon 13}$-*X*)GWTLNSAGYLLGKINLKALAALAKKIL-amide	1.00 ± 0.012	1.50 ± 0.03	0.22	353 ± 11
MAP *X*-KLALKLALKALKAALKLA-amide	1.70 ± 0.011	2.3 ± 0.04	0.31	484 ± 29

X = biotin or 2-nitro-tyrosinylcysteine.

were added to the wells to reach the final concentrations of 1, 5, 10 and 20 μM. As a positive control, some cells were treated with 1% Triton X-100 in PBS to establish the upper boundary of leakage. The plate was incubated at 37°C for 1 min after the addition of peptide, after which a 50-μl aliquot was transferred to a scintillation vial for quantification of 2-[^{3}H]deoxyglucose-6-phosphate leakage. The procedure was repeated after 5, 15 and 30 min, after which the remainder of the incubation solution (800 μl) was collected. The cells were dissolved by incubation in 0.5 ml of 1 M NaOH for 15 min. The base was transferred to scintillation vials and the wells were rinsed with 0.5 ml 1 M HCl. The acid fraction was used to neutralize the base fraction and the collected radioactivity in the combined fractions was measured in a β-scintillation counter (Packard, USA). The relative radioactive efflux from each well was calculated as percentage of control.

2.10. Calculation of mean μ

The mean μ [16] of the CPPs was calculated using the Kyte and Doolitle scale of hydrophobicity and a sliding window of nine amino acids on Winpep Software [17].

3. Results

The uptake and/or delivery of CPP–S–S–cargo fluorophore–quencher construct was measured as an increase in fluorescence using an energy transfer quenching method described by Meldal and Breddam [18] with some modifications. In order to measure the intracellular reduction rate constants, the constructs at 1 μM were reduced with various concentration of glutathione ranging from 100 μM to 2 mM. As the constructs probably are adsorbed to membranes also in the interior of the cells, the reduction was made in the presence of an excess of lipid vesicles. The observed reduction rate constants (k_2) are summarized in Table 1.

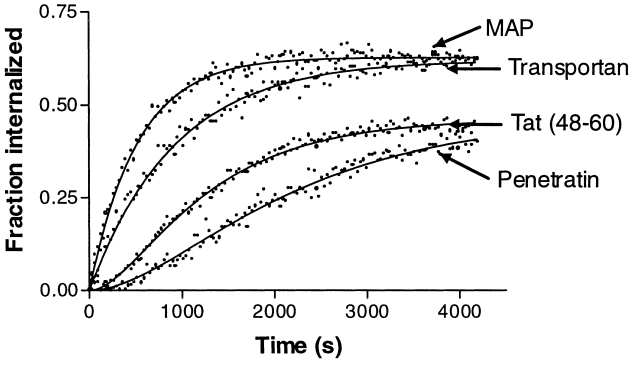

Fig. 2. Example illustrating uptake curves; uptake of fluorescence–quencher construct at 1 μM concentration expressed as fraction of total amount of construct plotted versus time. 1 is defined as the fluorescence intensity obtained after total reduction of constructs with DTT.

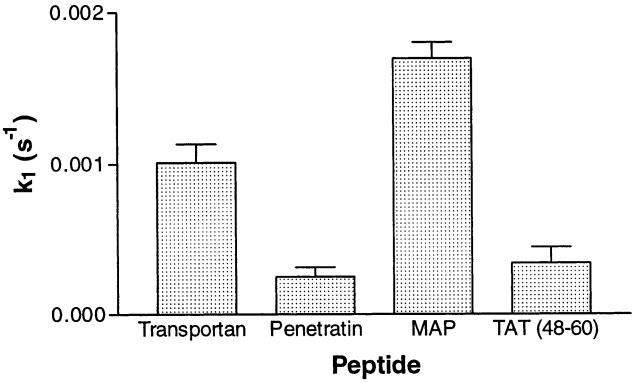

Fig. 3. The uptake rate constants (k_1) ± S.E.M. of the different fluorophore–quencher constructs used in this study.

The glutathione concentration in Bowes cells was determined to be 5.5 ± 0.4 mM, and this value was used in the fitting of the uptake data.

To confirm that the cargo peptide could not be internalized after extracellular reduction of the construct, independent uptake experiments were performed with the unconjugated cargo peptide. After 60 min incubation, no significant uptake could be measured.

To ascertain that the increase in fluorescence is not caused by glutathione outflow due to peptide-induced membrane leakage, cells were incubated in 5 μM of the inactive [Pro^{19}]transportan construct together with 10 μM of the biotinyl–MAP, the peptide showing most membrane disturbance (cf. below, Fig. 5). Only modest (< 1% of total) fluorescence increase above baseline was detected (data not shown). This experiment also excludes the possibility that unspecific interaction with extracellular proteins would enhance the reduction significantly.

As a further control, cells and constructs were mixed and immediately reduced with DTT. The resulting fluorescence intensity was similar to that ob-

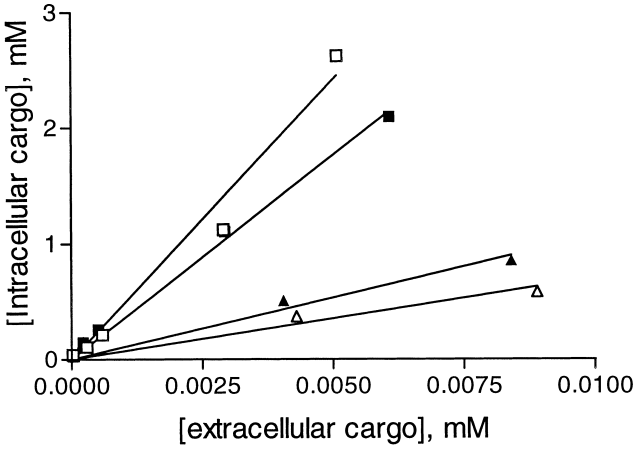

Fig. 4. Intracellular concentration of the fluorophore plotted against the extracellular concentration. The slope of the line determines the equilibrium constant, K_{io}.

tained at the end of the uptake experiments, showing that the observed uptake plateau is not due to quenching of the fluorophore intracellularly. An example of the uptake curves is illustrated with the curve for 1 μM of construct in Fig. 2. The uptake curves for all concentrations were simultaneously fitted using the Dynafit program package using the independently measured k_2 and intracellular glutathione concentration. This procedure showed that MAP had the fastest uptake ($k_1 = 1.7 \times 10^{-3}$ s^{-1}), followed by transportan ($k_1 = 1 \times 10^{-3}$ s^{-1}), Tat (48–60) ($k_1 = 0.34 \times 10^{-3}$ s^{-1}), and penetratin ($k_1 = 0.2 \times 10^{-3}$ s^{-1}). The uptake rate constants are summarized in Fig. 3 and table 1.

In Fig. 4, the estimated intracellular concentration at saturation (total intracellular volume 0.375 μl for 250 000 cells) is plotted against the extracellular concentration. The apparent cellular transport equilibrium constant (K_{io}) is obtained from the slope of the line (table 1). The linear dependence shows that the upper limit of the construct import (saturation) was not reached within the concentration range used. The CPPs seem to divide into two groups: group 1: MAP ($K_{io} = 417$) and transportan ($K_{io} = 353$); that possess higher delivery efficiency than group 2: Tat (48–60) ($K_{io} = 107$) and penetratin ($K_{io} = 71$). Thus, in all construct concentrations tested, transport stopped before 100% of the construct was internalized.

According to the 2-[^{3}H]deoxyglucose-6-phosphate leakage assay, MAP is the most potent inducer of membrane leakage, causing high outflow of radioactivity already at 1 μM concentration (Fig. 5). Higher concentrations of this peptide totally disrupt the cell plasma membranes and the leakage is comparable to the positive control, 1% Triton X-100 (data not shown). Tat (48–60) did not induce any detectable

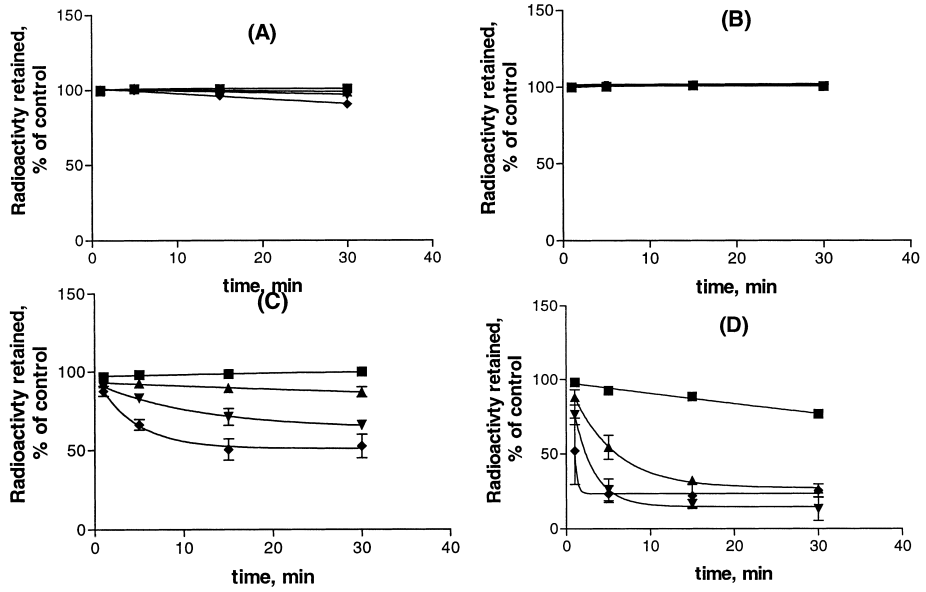

Fig. 5. Relative permeability of Bowes melanoma cells preloaded with 2-deoxyglucose, points are expressed as radioactivity retained in cells in % of non-treated cells. (A) penetratin, (B) Tat (48–60), (C) transportan and (D) MAP. Filled square = 1 μM, filled triangle = 5 μM, filled inverted triangle = 10 μM and filled diamond = 20 μM.

leakage at all, even at the highest concentration used (20 μM). Only a negligible effect was detected for penetratin: after 30 min of incubation with 20 μM the 90% of basal level radioactivity was retained in the cells (Fig. 5). Penetratin at lower concentrations induces less membrane leakage in a dose-dependent manner. Transportan had no effect at 1 μM but at higher concentrations the membrane leakage increased. Bowes cells incubated with 20 μM transportan for 15 min retained about 45% of basal radioactivity (Fig. 5).

4. Discussion

By using CPP–S–S–cargo constructs where the cargo is labelled with the Abz fluorophore and the CPP with the 3-nitrotyrosine quencher (Fig. 1), it is possible to monitor (in real time) the intracellular degradation of the disulfide bond, and hence the cellular uptake of the constructs by increase in apparent fluorescence intensity.

In order to calculate the uptake rate constants (k_1), the reduction rate constant (k_2) was first measured in experiments where the CPP–S–S–cargo constructs were exposed to varying concentrations of glutathione (Table 1). Since the amount of cells was kept constant throughout the experiments, the cellular uptake was modelled as a pseudo-first-order process while the reduction was modelled as a second order reaction. Hence, the uptake curves were numerically fitted to:

$$[\text{Construct}_{\text{extracellular}}] \xrightarrow{k_1} [\text{Construct}_{\text{intracellular}}]$$

$$[\text{Construct}_{\text{intracellular}}] + [\text{Glutathione}] \xrightarrow{k_2} [\text{Free cargo}]$$

with the maximum concentration of free cargo set to the intracellular endpoint concentration.

From earlier measurements of the uptake kinetics of transportan [5] it has not been clear whether a transmembrane equilibrium is involved in the transport process, or if the cells are saturated with the peptide. For the Tat (48–60) and penetratin peptides, no outflow from incubated cells has been measured [19,20], arguing that these peptides are not in a transmembrane equilibrium. However, for labelled transportan [5] and MAP [6], an outflow of label has been measured, but it is not clear if it is the intact peptide or metabolites that are exported.

Recalculated data from our previous work [11] show that the accumulation of the transportan and penetratin peptides in Bowes cells is 123- and 60-fold respectively. Thus, the value for the penetratin construct (Table 1) is similar to the peptide itself while for transportan, the intracellular cargo concentration is 4-fold higher than for the transporter peptide, implying that transportan is in an equilibrium over the membrane while penetratin is not.

In this experimental setup, an unrestricted equilibrium over the plasma membrane would drive the reduction of the construct to completion, ending at an uptake of 100% of available label as the labile nature of the disulfide bond lead to dissociation of the quencher and the fluorophore once the construct has entered the cells. However, dependent of construct and construct concentration, between 12 and 90% of the total amount of the constructs was internalized. The lack of complete uptake indicates that some equilibrium conditions must exist in the cellular uptake process, but, as mentioned, it should not be primarily over the plasma membrane. Consequently, the inhibition of uptake that results in a plateau must take some other form.

Recently Bellet-Amalric et al. showed that model membranes are quickly saturated with penetratin [21]. It would be reasonable to speculate that this is the case for the plasma membrane as well. Moreover, in cells, the peptide in the outer leaflet is transported into the cell where an equilibrium between cytosolic and membrane-bound peptide should be established. In the uptake process, the intracellular and membrane concentration of the peptide increases. At the endpoint, the membrane would be saturated with peptide and this would prevent further import. This is supported by a previous study showing that after the membrane potential-dependent uptake of a small positively charged amphipathic peptide into artificial vesicles [22] the peptide accumulates in the inner leaflet interface. This would explain why uptake stops apparently without equilibrium over the plasma membrane. The proposed process is illustrated in Fig. 6.

The difference in cargo delivery efficiency between the two groups of CPPs could be explained by the ability of the amphipathic transportan–MAP group

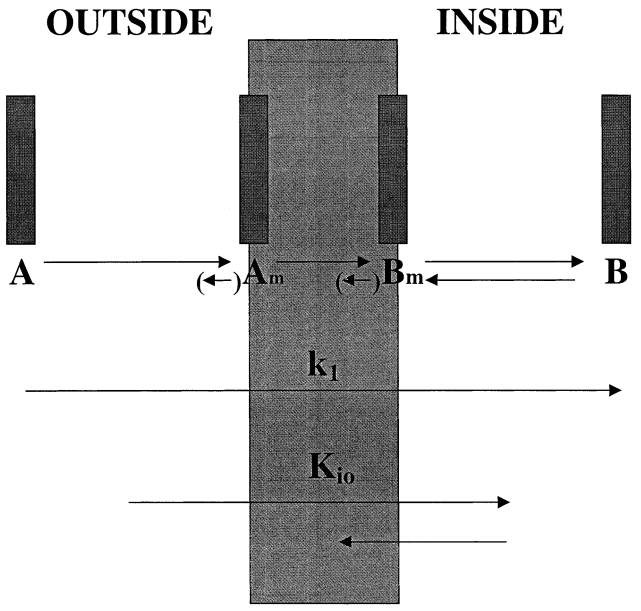

Fig. 6. Kinetic model of CPP uptake; the peptide in solution (A) is in equilibrium with peptide bound to the outer leaflet (A_m), which then translocates the plasma membrane. Inside the cell, the membrane-bound peptide (B_m) is in equilibrium with cytoplasmic peptide (B). The uptake rate constants (k_1) measured in this work would then correspond to the overall rate constant for the process and K_{io} should be the equilibrium constant. The construct uptake stops due to build-up of the liberated transporter peptide in the membrane.

of peptides to enter and exit cells, in contrast to the Tat (48–60)-penetratin group which are trapped in the cells.

Previously we have measured uptake of radio-iodinated transportan [5]. However, the fitting used considered an equilibrium over the membrane giving an overall (k_1+k_{-1}) rate constant of 2.8×10^{-3} s^{-1}. This is higher than the constant measured for the transportan construct in this work ($k_1 = 1\times10^{-3}$ s^{-1}), suggesting that, at least for the transportan construct, the added cargo decrease the uptake rate. Furthermore, a study on cells treated with transportan conjugated to gold particles showed that the complexes are residing both in vesicular structures and the cytoplasm [23], suggesting that for large transportan–cargo complexes, endocytosis occurs side-by-side with the cell-penetrating process. Thus, the delivery process appears to consist of two competing mechanisms: the fast cellular penetration and the 'normal', slower, endocytosis. From this it seem reasonable to conclude, at least for transportan, that the rate of cell penetration decreases with larger cargo, while that of endocytosis is more or less constant.

However, the kinetic constants are probably dependent not only on the peptides, but also on the membrane area as well as the lipid composition of the cell membrane, and consequently will vary with the cell-line used.

The glucose analogue, 2-deoxyglucose, is taken up into cells by glucose transporters and is phosphorylated inside the cells by hexokinase. The product, 2-deoxyglucose-6-phosphate, cannot leave the cell via the plasma membrane [14]. Thus, the efflux of radioactivity from cells preloaded with tritium-labelled 2-deoxyglucose requires some form of membrane disturbance. The μ of a peptide is a measure of its amphipaticity and has been implied as an important factor in peptide-mediated membrane disturbance. As can be seen from Fig. 7, the leakage seems to be linearly dependent of the mean μ of the peptides used. The relationship between the percentage of retained radioactivity (R) and μ can be empirically defined as $R = 120–293\ \mu$. This is supported by a study by Wieprecht et al., showing that the even slight changes in μ of melittin analogues have profound effects on the membrane permeabilization by the peptides [24].

In conclusion, there are two classes of CPPs. The first class consisting of amphipatic helical peptides where Lys is the main contributor to the positive charge. The representatives of this class, MAP and transportan cause membrane leakage at lower con-

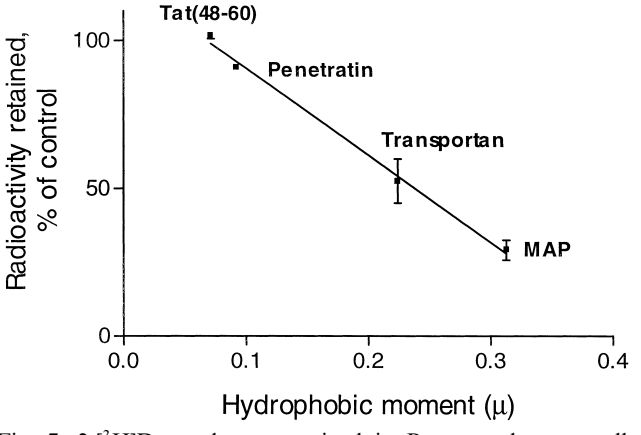

Fig. 7. 2-[^{3}H]Deoxyglucose retained in Bowes melanoma cells after a 30-min treatment with 20 μM peptide, plotted against the μ of the peptide, showing the correlation between membrane leakage and amphipathicity.

centrations and deliver more cargo into the cells than the representatives of the second class: the Arg rich Tat (48–60) and penetratin. Peptides of the first class are in equilibrium over the membrane while members of the second class are not.

The peptide-induced membrane leakage seems to be proportional to μ. Thus, in the design of novel CPP analogues, μ should be minimized in order to decrease the CPP-induced plasma membrane damage.

Acknowledgements

The authors wish to thank Professor Matjaz Zorko for fruitful discussion. This work was supported by Grants from the Swedish Council for Natural Science (NFR), the Swedish Council for Engineering Sciences (TFR) and EC Biotechnology Project BIO4–98-0227.

References

[1] M. Lindgren, M. Hällbrink, A. Prochiantz, Ü. Langel, Trends Pharmacol. Sci. 21 (2000) 99–103.
[2] A. Scheller, J. Oehlke, B. Wiesner, M. Dathe, E. Krause, M. Beyermann, M. Melzig, M. Bienert, J. Pept. Sci. 5 (1999) 185–194.
[3] D. Derossi, A.H. Joliot, G. Chassaing, A. Prochiantz, J. Biol. Chem. 269 (1994) 10444–10450.
[4] E. Vivès, P. Brodin, B. Lebleu, J. Biol. Chem. 272 (1997) 16010–16017.
[5] M. Pooga, M. Hällbrink, M. Zorko, Ü. Langel, FASEB J. 12 (1998) 67–77.
[6] J. Oehlke, A. Scheller, B. Wiesner, E. Krause, M. Beyermann, E. Klauschenz, M. Melzig, M. Bienert, Biochim. Biophys. Acta 1414 (1998) 127–139.
[7] D. Derossi, G. Chassaing, A. Prochiantz, Trends Cell. Biol. 8 (1998) 84–87.
[8] S.R. Schwarze, S.F. Dowdy, Trends Pharmacol. Sci. 21 (2000) 45–48.
[9] M. Pooga, U. Soomets, M. Hällbrink, A. Valkna, K. Saar, K. Rezaei, U. Kahl, J.X. Hao, X.J. Xu, Z. Wiesenfeld-Hallin, T. Hökfelt, T. Bartfai, Ü. Langel, Nat. Biotechnol. 16 (1998) 857–861.
[10] U. Soomets, M. Lindgren, X. Gallet, M. Hällbrink, A. Elmquist, L. Balaspiri, M. Zorko, M. Pooga, R. Brasseur, Ü. Langel, Biochim. Biophys. Acta 1467 (2000) 165–176.
[11] M. Lindgren, X. Gallet, U. Soomets, M. Hällbrink, E. Bråkenhielm, M. Pooga, R. Brasseur, Ü. Langel, Bioconjug. Chem. 11 (2000) 619–626.
[12] Ü. Langel, T. Land, T. Bartfai, Int. J. Pept. Protein Res. 39 (1992) 516–522.
[13] P. Kuzmic, Anal. Biochem. 237 (1996) 260–273.
[14] D.E. Smith, J. Gorski, J. Biol. Chem. 243 (1968) 4169–4174.
[15] E. Walum, A. Peterson, Anal. Biochem. 120 (1982) 8–11.
[16] D. Eisenberg, E. Schwarz, M. Komaromy, R. Wall, J. Mol. Biol. 179 (1984) 125–142.
[17] L. Hennig, Biotechniques 26 (1999) 1170–1172.
[18] M. Meldal, K. Breddam, Anal. Biochem. 195 (1991) 141–147.
[19] S. Futaki, T. Suzuki, W. Ohashi, T. Yagami, S. Tanaka, K. Ueda, Y. Sugiura, J. Biol. Chem. 276 (2001) 5836–5840.
[20] G. Drin, M. Mazel, P. Clair, D. Mathieu, M. Kaczorek, J. Temsamani, Eur. J. Biochem. 268 (2001) 1304–1314.
[21] E. Bellet-Amalrica, D. Blaudezb, B. Desbatc, F. Granerd, F. Gauthierd, A. Renaultd, Biochim. Biophys. Acta 1467 (2000) 131–143.
[22] A.I. de Kroon, B. Vogt, R. van't Hof, B. de Kruijff, J. de Gier, Biophys. J. 60 (1991) 525–537.
[23] M. Pooga, C. Kut, M. Kihlmark, M. Hällbrink, S. Fernaeus, R. Raid, T. Land, E. Hallberg, T. Bartfai, Ü. Langel, FASEB J. 15 (2001) 1451–1453.
[24] T. Wieprecht, M. Dathe, E. Krause, M. Beyermann, W.L. Maloy, D.L. MacDonald, M. Bienert, FEBS Lett. 417 (1997) 135–140.